Quaternary International 304 (2013) 183–192

Contents lists available at SciVerse ScienceDirect

Quaternary International

journal homepage: www.elsevier.com/locate/quaint

Climatic variability in Central Indian Himalaya during the last ~1800 years: Evidence from a high resolution speleothem record

Jaishri Sanwal [a], Bahadur Singh Kotlia [b,*], Chittenipattu Rajendran [a], Syed Masood Ahmad [c], Kusala Rajendran [a], Mike Sandiford [d]

[a] Centre for Earth Sciences, Indian Institute of Science, Bangalore 560 012, India
[b] Centre of Advanced Study in Geology, Kumaun University, Nainital 263 002, India
[c] National Geophysical Research Institute (CSIR), Hyderabad 500 007, India
[d] Department of Geological Sciences, University of Melbourne, Melbourne, Australia

ARTICLE INFO

Article history:
Available online 27 March 2013

ABSTRACT

Stable isotopes from a U/Th dated aragonite stalagmite from the Central Kumaun Himalaya provide evidence of variation in climatic conditions in the last ~1800 years. The $\delta^{18}O$ and $\delta^{13}C$ values vary from −4.3‰ to −7.6‰ and −3.4‰ to −9.1‰ respectively, although the stalagmite was not grown in isotopic equilibrium with cave drip water, a clear palaeoclimatic signal in stalagmite $\delta^{18}O$ values is evident based on the regional climate data. The stalagmite showed a rapid growth rate during 830–910 AD, most likely the lower part of Medieval Warm Period (MWP), and 1600–1640 AD, the middle part of Little Ice Age (LIA). Two distinct phases of reduced precipitation are marked by a 2‰ shift in $\delta^{18}O$ values towards the end of MWP (~1080–1160 AD) and after its termination from ~1210 to 1440 AD. The LIA (~1440–1880 AD) is represented by sub-tropical climate similar to modern conditions, whereas the post-LIA was comparatively drier. The Inter Tropical Convergence Zone (ITCZ) was located over the cave location during wetter/warmer conditions. When it shifted southward, precipitation over the study area decreased. A prominent drop in $\delta^{18}O$ and $\delta^{13}C$ values during the post-LIA period may also have been additionally influenced by anthropogenic activity in the area.

1. Introduction

The Indian monsoon is a major weather system on Earth and variations in its intensity have widespread socio-economic impacts. Despite dedicated efforts by scientists over the centuries, a comprehensive picture of variability in the Indian Summer Monsoon (ISM) and Westerlies for the Indian Himalayan sector has been elusive, especially on the time scales relevant to society. The absence of quantitative, long term high resolution (multi-annual to decadal) records and complexity and multiplicity of factors influencing the Indian Summer Monsoon have hindered the efforts to understand the behaviour of ISM and Westerlies in the Himalaya. This issue needs to be addressed, because any changes in the nature of the influencing factors or the magnitude of their impact (e.g., severity of droughts and floods) are critical for land-use planning in a global warming scenario. The Himalaya not only influences the rainfall pattern in India, but also obstructs the path of the cold winds from the north because of altitude and location. The Inner Asian high pressure systems and winter Westerlies are the main components of Himalayan climate, and a combined impact of rainfall, latitude, and altitude controls climate patterns. The region mainly experiences two seasons tied to the summer and winter monsoons, with precipitation generally recorded during June to September that decreases from east to western Himalaya. The east–west variation is based on the dominance of different weather systems, which in turn cause the monsoon to weaken from east to west. As the response of the ISM and rainfall over the Himalaya have not been completely linear (Overpeck et al., 2005), the dual monsoon system (summer and winter monsoons) over the sub-continent has a distinctly different origin and dynamics (Sarkar et al., 2000). The monsoon precipitation is mainly of an orographic nature, resulting in distinct variations in rainfall with elevation between the southern slopes of the Himalayas and the rain shadow areas on the Tibetan Plateau. The extreme relief of the Himalaya yields a marked change in air masses crossing the region and results in a complex mosaic of "topo-climates" (Alford, 1992). These range from the sub-tropical climate in the foothills, to the

* Corresponding author. Department of Geology, Kumaun University, Durham House, Tallital, Nainital 263002, Uttarakhand, India.
E-mail address: Bahadur.kotlia@gmail.com (B.S. Kotlia).

1040-6182/$ – see front matter © 2013 Elsevier Ltd and INQUA. All rights reserved.
http://dx.doi.org/10.1016/j.quaint.2013.03.029

temperate climate in the middle hills and alpine climates in the high mountains. Therefore, Himalayan climate records display a great variability, and are not representative of the precipitation over the entire Indian region. Meteorological data for the last about 130 years from one of the oldest stations in Central Indian Himalaya (Kotlia et al., 2012) show that 15–20% of the annual precipitation is contributed by the Westerlies, and thus their role cannot be overlooked while using any proxy for the past climatic changes in the Central Indian Himalaya. Moreover, no major changes in orographic elevation in the region due to tectonics are expected during the last 2000 years which would have an impact on the direction of the Westerlies.

Although the data on rainfall intensity of ISM during the Holocene are reported from a number of marine and lacustrine sediments (Sirocko et al., 1993; Gasse et al., 1996; Prasad et al., 1997; Schulz et al., 1998; Sarkar et al., 2000; Staubwasser et al., 2003), their temporal resolution is low and the chronological accuracy is insufficient to resolve decadal or multi-annual scale variability. High-resolution marine records from the Arabian Sea track wind strength and coastal upwelling and indicate stronger early and mid-Holocene summer monsoon winds (Overpeck et al., 1996; Sirocko et al., 1996; Gupta et al., 2003; Jung et al., 2004) but cannot be expected to serve as proxies for Himalayan climate. There are two major drawbacks of marine records which limit their usefulness for modeling studies: (i) periods of increased monsoon wind strength inferred from marine records do not always coincide with increased precipitation over nearby continental regions; and (ii) the vast majority of marine records have at best centennial-scale resolution. From Indian Himalaya itself, the scattered, inconsistent and very poorly dated Holocene records from the terrestrial deposits (Sharma and Gupta, 1995, 1997; Phadtare, 2000; Ranhotra et al., 2001; Gupta, 2002, 2008; Kar et al., 2002; Chakraborty et al., 2006; Chauhan, 2006; Phadtare and Pant, 2006; Rühland et al., 2006; Kotlia et al., 2010; Rawat et al., 2012) show only millennial scale climatic changes and do not reflect the decadal scale changes. Although scattered and sporadic, the evidence of millennial-scale climate events in the Late Holocene lake/peat deposits are preserved in northern India but chronological control on these time series is weak.

Long term precipitation and temperature variations spanning the last ~2000 years have been studied by a number of workers (Jones et al., 1998; Briffa, 2000; Crowley and Lowery, 2000; Esper et al., 2002; Cook et al., 2003; Mann and Jones, 2003; Mann et al., 2008, 2009; Jones and Mann, 2004; Moberg et al., 2005; D'Arrigo, 2006; Osborn and Briffa, 2006; Loehle, 2007; Hegerl et al., 2007; Juckes et al., 2007; Ljungqvist, 2010). This period contains two significant episodes of climatic change: the warming period known as the MWP (~900–1300 AD) and the relatively cold LIA (~1500–1850 AD). However, MWP and LIA seem to be restricted to the circum-North Atlantic region (Hughes and Diaz, 1994; Mann et al., 1999; Mann and Jones, 2003) and do not appear to have occurred synchronically in other regions (Grove, 1988) largely due to substantial uncertainty of the inception and duration of these episodes in different parts of the globe (Bradley, 1992; Bradley and Jones, 1993). The intensity of the ISM is generally considered to have weakened during the LIA (Anderson et al., 2002; Gupta et al., 2003), but there is also evidence of wetter conditions during the LIA in the Indian Himalaya (Rühland et al., 2006; Kotlia et al., 2012), Nepal (Denniston et al., 2000) and the sites falling within the similar latitudes (e.g., Chu et al., 2002; Chen et al., 2005). In order to better understand the behaviour of past climatic events in the Himalaya during MWP and LIA, we developed a high-resolution stable isotopic record from a precisely-dated stalagmite from Dharamjali cave (district Pithoragarh) in the east Uttarakhand Himalaya. Drivers of variability of the Westerlies have received much less attention than ISM rainfall, especially in the Himalaya. In this region, the winter rains (Westerlies) contribute a considerable amount of the total annual rainfall, allowing a rare examination of variability of the Westerlies over the late Holocene.

2. Cave site

Dharamjali cave (29°31′27.8″N: 80°12′40.3″ E; altitude 2200 m, see Fig. 1) is developed in Precambrian Thalkedar Limestone, predominantly structureless blue calcitic limestone, interbedded with dolomitic (cherty) limestone and dolomite (Valdiya, 1980). The cave lies approximately 50 m below the land surface, which is capped by a 1–2 m-thick brownish black topsoil, mostly made up of A horizon which includes organic matter (fallen leaves and twigs) and forms humus. The two chambered and sub-vertical cave is about 35 m long, becoming very narrow in the last chamber (entrance about 0.8 × 0.9 m) where the evaporation effect is minimal. The cave is wet throughout the year with water dripping around the center of cave at a rate of 20–30 drops/min. during the monsoon and 3–8 drops/min. during the winter. Inside the cave, the humidity ranges between 50 and 70%, and the temperature ranges from 8–15 °C (data collected in 2009). The annual precipitation in the area is ~1200–1400 mm with about 80% of the precipitation falling during the monsoon season from May to September. The Westerlies contribute about 15–20% of the total annual precipitation. The vegetation in the surrounding area is composed predominantly of moisture-loving Oak (*Quercus*), *Rhododendron*, *Pinus roxburghii* with small shrubs, grasses, ferns and herbs. The climate is subtropical with wetter and warmer summers and drier and cooler winters. The sample (DH-2) was collected (November, 2010) from the near end, about 33 m away from the main entrance, and was active.

3. Methodology

DH-2 is a 17.5-cm-long aragonite stalagmite, the chronology for which was developed using five U/Th dates (Table 1) obtained using Multi Collector-Inductively Coupled Plasma Mass Spectrometry (MC-ICP-MS) at the University of Melbourne, Australia. Powdered samples were extracted by using a 1 mm drill bit driven by a micro-milling lathe. The samples were dissolved in HNO_3 and spiked with a mixed $^{229}Th/^{233}U$ tracer, followed by matrix separation using ion exchange chromatography in which U and Th were collected as a single cut. The U and Th isotope ratios were determined simultaneously using the parallel ion counting technique of Hellstrom (2003). The large age uncertainty in the sample MS-1 perhaps stems from uncertainty in the initial Th isotopic composition. The estimate of 0.75 ± 0.50 (see Table 1) is a derived approximation, most likely in Bayesian analysis (see Hellstrom, 2006). Calibration of dates used the model StalAge (Fig. 2) following Scholz and Hoffmann (2011). The StalAge seems to be a more realistic age and allows understanding of the precise variation in the sample growth in different sectors. Linear interpolation between the dates has not been used because it seems unlikely that the change in the growth rate took place exactly at the dating spots. Nevertheless, the StalAge model is the most useful age model. U/Th dating has yielded ages in calendar years (cal. year 2010) and the reference year for all ages given in the study is 2010 AD. The tip of the stalagmite is considered as zero years since it was active when collected.

A petrographic microscope with digital imaging facility (Olympus BX51 U-CMAD3) was used for preparing the thin sections at various depths of the sample. Both petrography and SEM studies were carried out in the Indian Institute of Science, Bangalore.

Isotopic measurements used the central-most part of the sample to avoid possible kinetic fractionation. A total of 219 samples

Table 1
U/Th dates in DH-2 stalagmite. The large error in MS-1 may be a result of uncertainty in Th included in the sample from dust, likely blown from outside the cave, as opposed to Th derived from U decay in the calcite from precipitation.

Sample	Depth (cm)	U (ngg^{1})	$[^{230}Th/^{238}U]$[a]	$[^{234}U/^{238}U]$[a]	$[^{232}Th/^{238}U]$	$[^{230}Th/^{232}Th]$	Age (ka)[b]	$[^{234}U/^{238}U]_i$[c]
MS-5	0.8	219	0.00573 (27)	1.7478 (35)	0.006149 (057)	0.9	0.07 (0.19)	1.7477 (35)
MS-4	5.44	443	0.00766 (18)	1.7454 (34)	0.000715 (009)	10.7	0.45 (0.03)	1.7462 (34)
MS-3	8.08	295	0.01785 (48)	1.7146 (33)	0.003784 (097)	4.7	0.97 (0.12)	1.7164 (33)
MS-2	16.96	986	0.0264 (37)	1.6522 (32)	0.000152 (002)	173.4	1.75 (0.03)	1.6554 (32)
MS-1	17.36	61	0.03744 (61)	1.6320 (40)	0.014968 (104)	2.5	1.78 (0.51)	1.6352 (41)

[a] Activity ratios determined after Hellstrom (2003) using decay constants of Cheng et al. (2000) (numbers in brackets are 2 SE uncertainties in the last significant figure).
[b] Ages in ka BP, corrected for initial ^{230}Th using Equation (1) of Hellstrom (2006) and $[^{230}Th/^{232}Th]_i$ of 0.75 ± 0.50 (numbers in brackets are 95% uncertainties).
[c] Initial $[^{234}U/^{238}U]$ calculated using corrected ages (numbers in brackets are 2 SE uncertainties in the last significant figure).

was analyzed for $\delta^{18}O$ and $\delta^{13}C$ values. The samples were milled with a regular interval of 0.8 mm along the central growth axis. About 50–60 μm g of powdered sample was used for isotopic measurements in a DeltaPlus Advantage Isotope Ratio Mass Spectrometer (IRMS), coupled with a Kiel-IV automatic carbonate device. This is a dual inlet device in which the sample is reacted in a vacuum system with H_3PO_4 at ~700 °C. This causes CO_2 to evaporate, which is trapped using Liquid Nitrogen at −190 °C. The isotopic compositions are reported in δ notation as per mil (‰) deviation from PDB standard. The analytical precision was better than 0.10‰ for $\delta^{18}O$ and 0.05‰ for $\delta^{13}C$. The calibration to the PDB standard was achieved by repeated measurements of international reference standards NBS-19 and NBS-18 (see Ahmad et al., 2008). Variations in growth rates of speleothems are caused by changes in

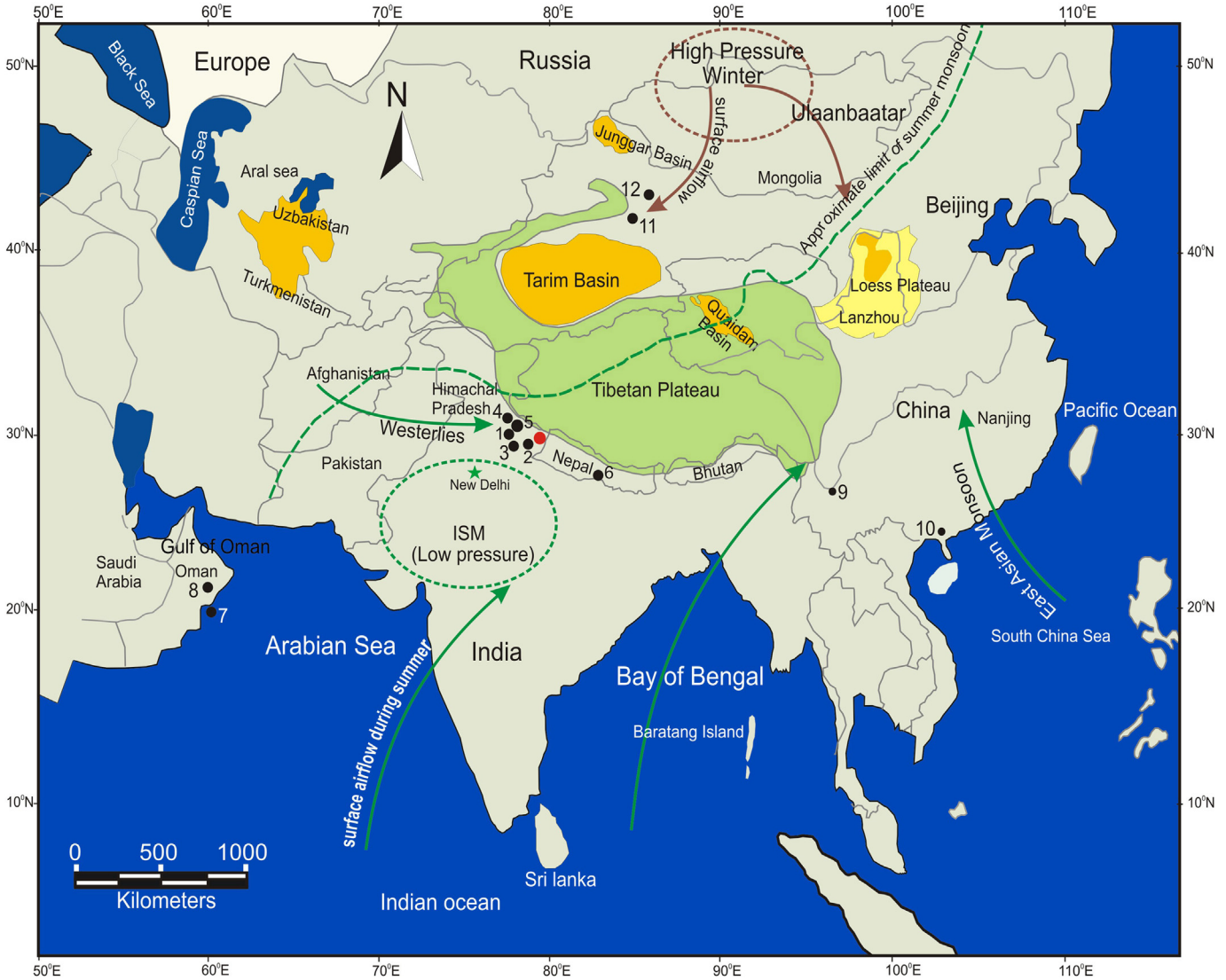

Fig. 1. Map of India and adjacent areas. Grey dot is DH-2 cave locality, and black dots represent other sites discussed in this work. Arrows indicate surface airflow during summer and winter with areas of high and low pressure (modified after Chen et al., 2009). 1. Chulerasim cave (Kotlia et al., 2012); 2. Timta cave (Sinha et al., 2005); 3. Nainital (Gupta, 2008); 4. Pinder valley (Rühland et al., 2006); 5. Western Himalaya (Singh and Yadav, 2005); 6. Sidha Baba cave (Denniston et al., 2000); 7. Arabian Sea (Gupta et al., 2003); 8. Oman (Fleitmann et al., 2004); 9. Erhai lake (Chen et al., 2005); 10. Huguangyan lake (Chu et al., 2002); 11. Bosten lake (Chen et al., 2006); 12. Xinjiang (Zhang et al., 2009).

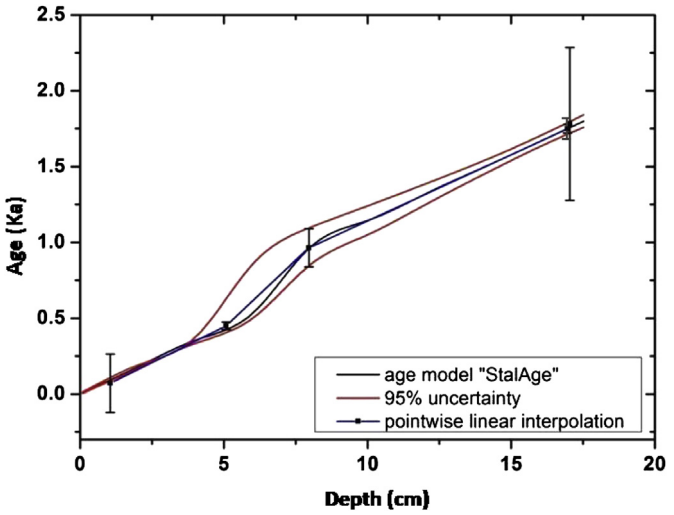

Fig. 2. Age–depth model (StalAge), following Scholz and Hoffmann (2011). Age of the top of sample is considered as zero as the stalagmite was active when cut in off monsoon period.

climate conditions (particularly precipitation), soil carbon dioxide concentration and temperature as well as calcium ion concentration of the drip-waters (Kaufmann and Dreybrodt, 2004; McDermott, 2004). Therefore, changes in growth rate accompanied with variations in $\delta^{18}O$ and $\delta^{13}C$ also offer a possibility of understanding the past climate changes.

4. Hendy test

DH-2 was collected from the last and a very small chamber, thereby reducing the chance that evaporation or kinetic fractionation impacted stable isotopic ratios. Five samples were measured along the length of one individual growth layer (4.1 cm from the top) to test the isotopic equilibrium with precipitating waters, following criteria outlined by Hendy (1971). The preliminary results (Fig. 3), as per this test, show that the sample was perhaps not grown under ideal equilibrium, but $\delta^{18}O$ can still be used as a dependable indicator of precipitation. As such, the Hendy test has two main criteria: (1) along a single growth layer, $\delta^{18}O$ shows little variations while $\delta^{13}C$ may vary irregularly; and (2) $\delta^{18}O$ and $\delta^{13}C$ values along a single growth are not positively correlated (Hendy and Wilson, 1968; Hendy, 1971; Schwarcz, 1986; Gascoyne, 1992). The practical limitations of this test are described by several researchers, and limitations of the test are described by Fleitmann et al. (2004), Webster et al. (2007), Dorale and Liu (2009), Daëron et al. (2011) and more recently by Zhou et al. (2011). These studies suggest that, (1) there is no absolute test for the absence of kinetic/vadose-zone processes; and (2) despite Hendy test failure, stalagmites can be used as proxies for precipitation, chiefly because $\delta^{18}O$ values of speleothem calcite primarily reveal rainfall rather than temperature. A number of workers (e.g., Talma and Vogel, 1992; Spötl and Mangini, 2002; Dreybrodt, 2008) have found that the Hendy test is not a perfect experiment for the presence of equilibrium conditions primarily because isotopic equilibrium can occur in the center of a stalagmite at the same time that kinetic fractionation occurs at the outer flanks. Subsequent studies on kinetic fractionation also showed that this test was not convincing in practice (Mickler et al., 2004, 2006; Dorale and Liu, 2009). While investigating the kinetic fractionation in three caves in Korea, Woo et al. (2006) concluded that the "Hendy Test" may not be appropriate due to the change in the supply rate of dripping water. They therefore proposed that different texture in stalagmites may be used as another criterion to determine the degree of equilibrium. Further, 44 years of $\delta^{18}O$ values for rainfall at New Delhi, ~300 km SW of the cave site, indicate that the precipitation during the monsoon period categorically has lighter $\delta^{18}O$ values (~−5.6‰ to −9.5‰) compared to that in the dry months (~−1.0‰ to −2.0‰, see Fig. 5 of Kotlia et al., 2012), indicating that $\delta^{18}O$ primarily indicates precipitation. To summarize, in sub-tropical areas, even if this test fails, $\delta^{18}O$ is still a very reliable indicator for precipitation (see Fleitmann et al., 2004; Zhou et al., 2011; Kotlia et al., 2012).

5. Results

Petrography (Fig. 4A–F) and SEM studies (Fig. 4G–I) reveal that the stalagmite is mostly composed of aragonite which has very elongated crystals, usually in botryoidal clusters (Fig. 4D–F). The common morphology of aragonite is acicular crystals (needle-like, straight, thin and markedly elongated) and pointed (Fig. 4D–I). Alternate layers are mostly composed of compact layers with a few porous layers, usually made up of large to small botryoidal clusters of aragonite (Fig. 4C–F) with occasional calcite. The compact layers are formed by well-developed elongated crystals (Fig. 4G–I) and are generally oriented parallel to the vertical growth axis. The porous and thin sub-layers are made up of drusy and fibrous aragonite. Thin sub layers of calcite show palisade fabric (Fig. 4C and E).

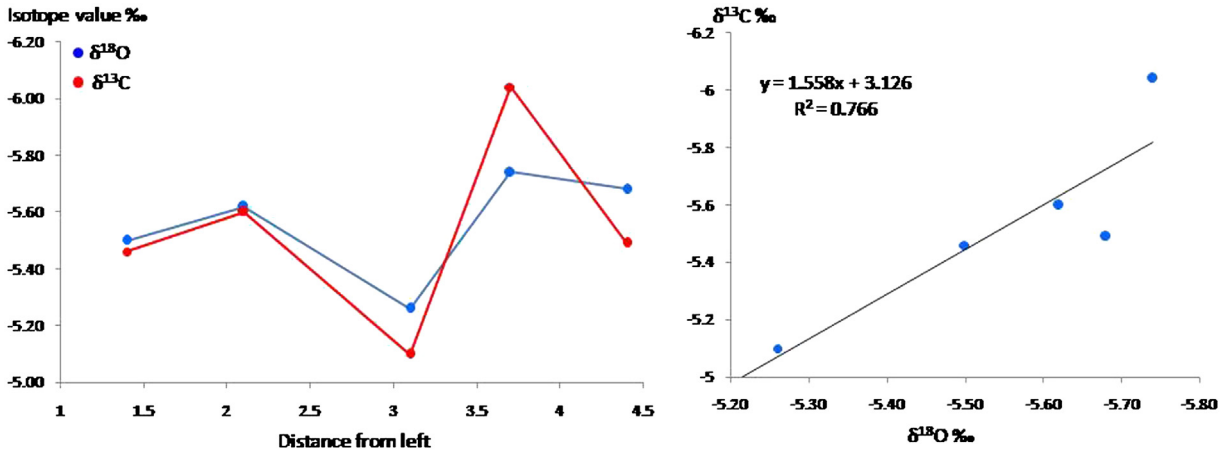

Fig. 3. Variations in $\delta^{18}O$ and $\delta^{13}C$ values along a single growth layer of the stalagmite (DH-2).

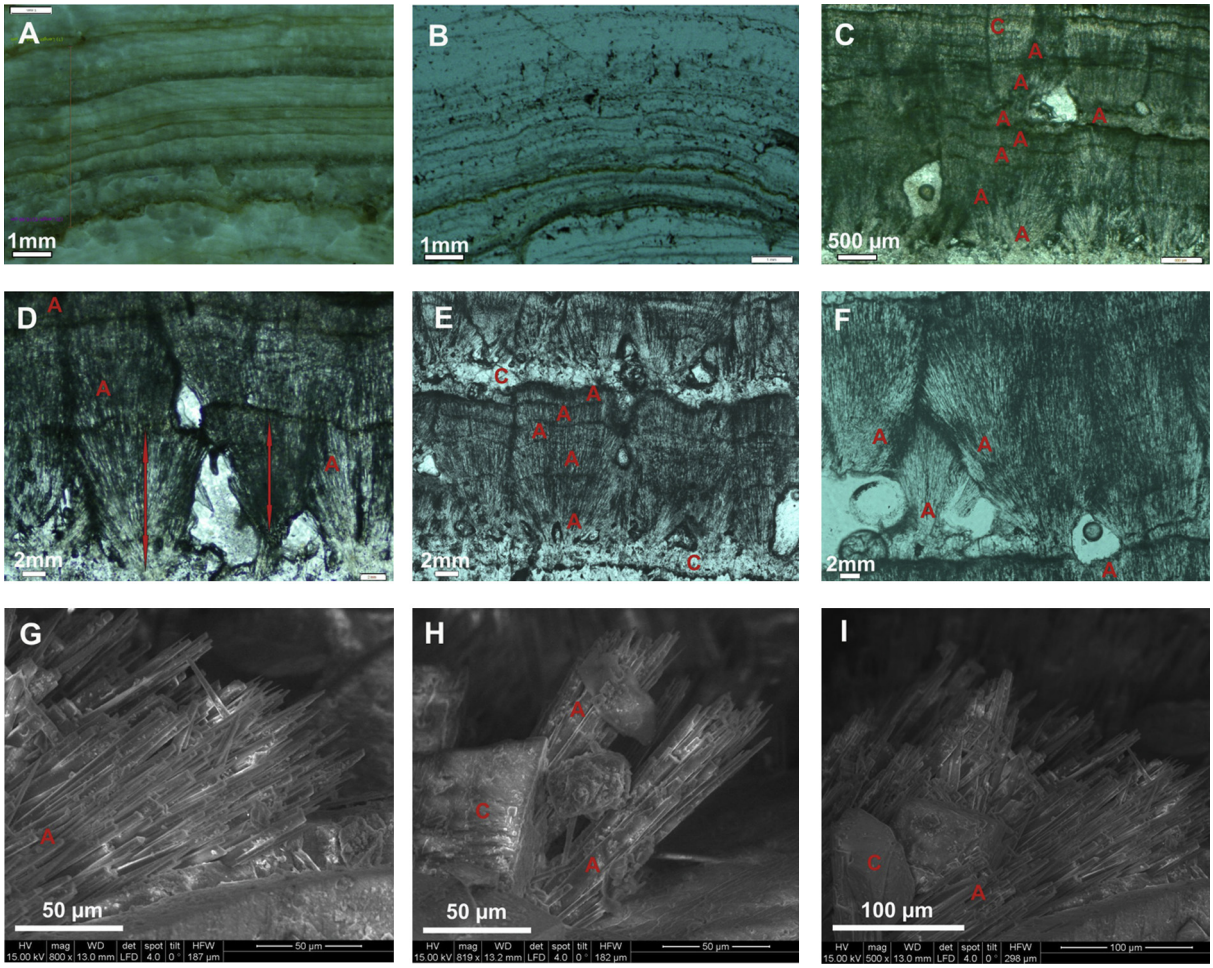

Fig. 4. Petrographic (A–F) and SEM (G–I) analyses of DH-2 stalagmite. (A), Polished surface of upper part of stalagmite showing multiple laminae as compact fabrication and porous layers under UV light; (B) Middle part showing laminae and sub laminae under plane polarized light; (C) Upper part under plane polarized light showing aragonite clusters (A) and a layer (C) of calcite; (D) Lower part with botryoidal clusters of aragonite under plane polarized light; (E) Middle part of stalagmite under plane polarized light showing multiple layers of botryoidal clusters of aragonite with two distinct layers of calcite; (F) Lower part showing fibrous aragonite under plane polarized light; (G) SEM image of upper part of stalagmite showing elongated columnar aragonite crystals, oriented parallel to the vertical growth axis; (H) Middle part of the sample with botryoids of aragonite with a small crystal of calcite; (I) Lower part of stalagmite showing needle like, straight, thin and markedly elongated crystals of aragonite.

DH-2 $\delta^{18}O$ and $\delta^{13}C$ values vary between −4.3‰ to −7.6‰ and −3.4‰ to −9.1‰ respectively and are similar to variations in precipitation (Fig. 5). The $\delta^{13}C$ of soil CO_2 is generally dependent on the vegetation above the cave, with lighter values where the plant cover is predominantly of C_3 type (average $\delta^{13}C$ of C_3 plants = −27‰) and heavier when C_4 plants (average $\delta^{13}C$ of C_4 plants = −14‰) (Osmond and Ziegler, 1975; Cerling, 1984) predominate. At present, the vegetation around DH-2 cave consists mainly of C_3 plants, and it is improbable that the plant cover has changed significantly in the last 1800 years. However, drier conditions in the past would have restricted plant growth and decreased the CO_2 in the soil above the cave. Stalagmite carbonate deposited under such conditions would have heavier $\delta^{13}C$ values. High CO_2 level in the soil above the cave is also one of basic conditions which must be met for speleothem growth to occur (Baker et al., 1993).

Generally, there is a positive correlation between drip rate and growth rate, although varying from locality to locality (Banner et al., 2007). Thus, the dry periods should be associated with lower or near-zero growth rates. The modeling of speleothems (see Banner et al., 2007) also envisages such a relationship. Therefore, the higher growth rate may be considered a result of the higher precipitation under wetter/warmer conditions. Some studies on the Holocene speleothem growth rates also support a positive linkage between drip rate and stalagmite growth (e.g., Genty et al., 2001). In this sample, noticeably lighter $\delta^{18}O$ values indicating the higher precipitation are also associated with higher growth rate.

Present day $\delta^{18}O$ values of the monsoonal drip water vary between −5.5‰ and −6.5‰ (Fig. 5) within the sub-tropical setting under warmer/wetter conditions. In general, there is a gradual enhancement in the precipitation from ~210 to 810 AD, and this long phase is punctuated by three multi-decadal dry events at 240–270 AD, 390–420 AD and 570–600 AD. The precipitation attained its maximum for about a century (~830–910 AD) during which the growth of the stalagmite was enhanced by almost three times (see Fig. 5). This segment may possibly be assigned to the lower part of MWP, and duration of MWP seems spanning from 830 to 1210 AD. However, towards the end of the MWP, a further distinct and multi-decadal dry event is observed from ~1080 to 1160 AD. Following the MWP, a pronounced phase from ~1210 to 1440 AD is represented by drier conditions, which is manifest in $\delta^{18}O$ values heavier by about 2‰. Additionally, this part is also characterized by almost minimum annual growth of the sample. The Little Ice Age (LIA) spans from ~1440 to 1880 AD with a comparatively wetter environment around the cave site. In addition to comparatively lighter $\delta^{18}O$ values, the stalagmite growth also increased in this sector (see

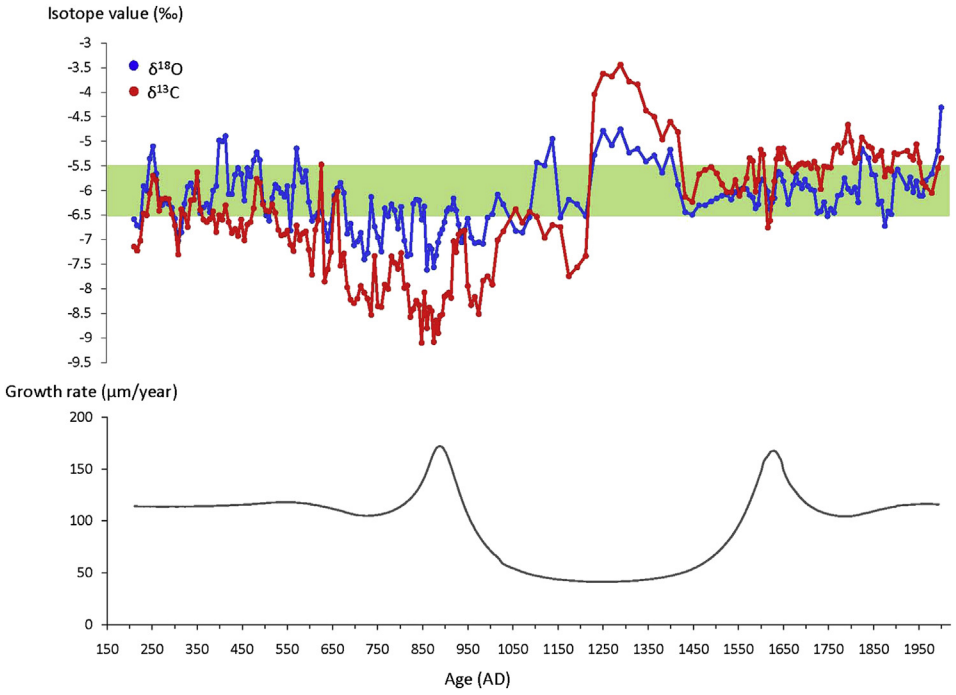

Fig. 5. $\delta^{18}O$ and $\delta^{13}C$ data along the central growth axis of DH-2 stalagmite. Background panel indicates the range of present day $\delta^{18}O$ values of drip water and lower curve shows growth rate.

Fig. 5). The post-LIA from ~1880 AD onwards was drier than the LIA, as the $\delta^{18}O$ values are distinctly heavier by about 2‰.

6. Comparison with other sites

The DH-2 record indicates that the MWP (generally from ~800 to 1200 AD) is characterized by an asymmetrical trend in $\delta^{18}O$ values. Based on the pollen and carbon isotopic studies of lake sediments in Paradise Alpine lake in northeastern Himalaya, Chauhan (2006) suggested a warmer and moister climate around 910 AD, similar to these results and probably corresponding to the MWP. Chen et al. (2006) examined the pollen and carbonate content of sediments from Bosten Lake, and concluded that the MWP was dry in south of Xinjiang (China). Zhang et al. (2009) proposed a humid climate in north Xinjiang. In a comprehensive study, Yang et al. (2002) used nine separate proxy climate records derived from peat, lake sediment, ice core and tree ring and other sources to compile a single weighted temperature history for all of China spanning the past two millennia. This record revealed warm conditions from 800 to 1400 AD (including Medieval Warm Period between 800 and 1100 AD). Therefore, the so-called MWP is manifestly diverse in different regions, and the climate may have varied in time and space during this period, as has been pointed out by Zhang et al. (2009) especially in the Tibetan Plateau and Xinjiang region. However, despite such variations in MWP, it is a major climate anomaly, which provides useful palaeoclimatic information. Perhaps "Medieval Climate Anomaly" should be a more suitable term than MWP (Stine, 1994; Diaz et al., 2011).

A change to lighter $\delta^{18}O$ values indicates increases in the intensity of precipitation between ca. 1440–1880 AD. This prominent signal may be ascribed to the LIA with stronger Westerlies and weaker ISM as was also documented by Kotlia et al. (2012). This is largely because the ISM has been weaker during this period in the Oman margin and Arabian Sea regions (Anderson et al., 2002; Gupta et al., 2003) and higher precipitation in the Himalayan foothills during the same time may be explained only by the stronger Westerlies. Fig. 6 shows the comparison in $\delta^{18}O$ and $\delta^{13}C$ values between Chulerasim (Kotlia et al., 2012) and DH-2 stalagmites. As both sites are located within similar precipitation regimes, the $\delta^{18}O$ values show similar trends. Additionally, comparison of DH-2 $\delta^{18}O$ with the annual rainfall (1897–2000) from Mukteshwar meteorological station (29°28′ N: 79°39′ E, altitude 2311 m, ~130 km SW of cave site) reveals a positive correlation (Fig. 7). However, a slight deviation may be ascribed to the elevation difference.

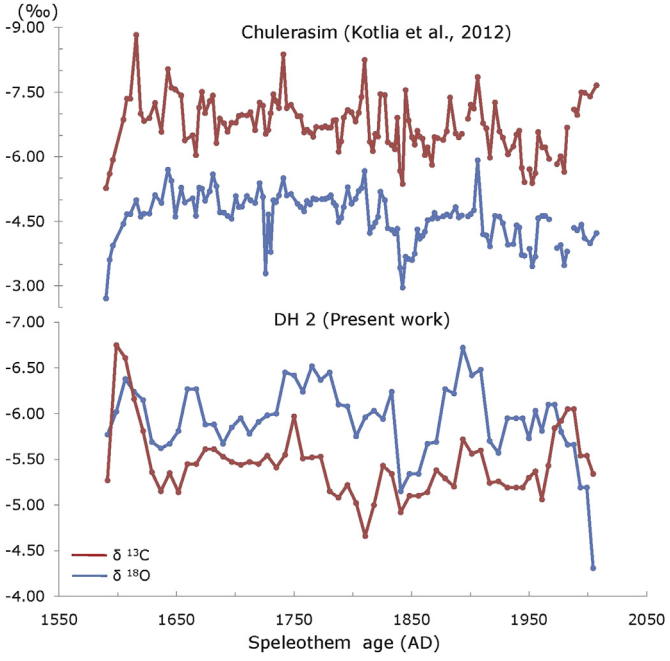

Fig. 6. Comparison of $\delta^{18}O$ and $\delta^{13}C$ values in Chulerasim (Kotlia et al., 2012) and DH-2 stalagmites. Both the sites fall within almost same precipitation regimes.

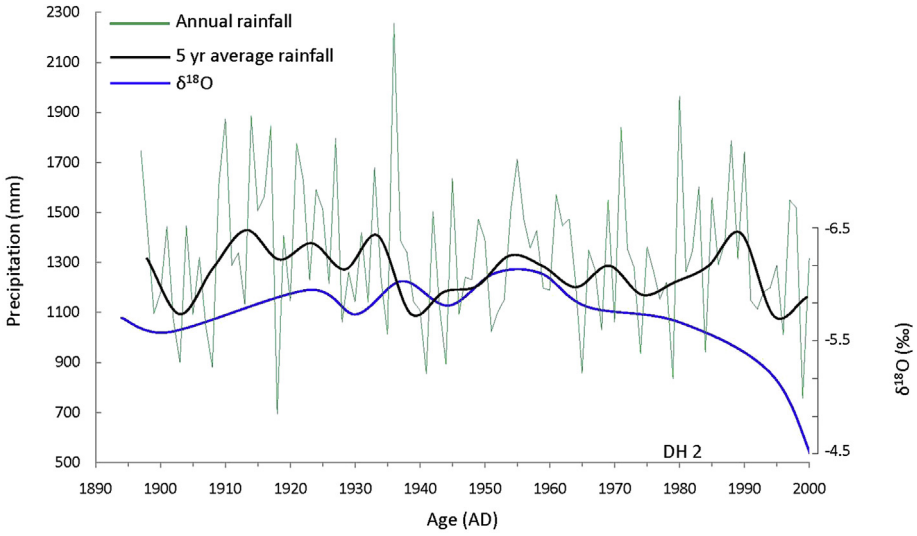

Fig. 7. Comparison of DH-2 $\delta^{18}O$ and rain fall data from Mukteshwar meteorological station (1897–2000 AD; Rainfall data from Indian Institute of Meteorology, Pune).

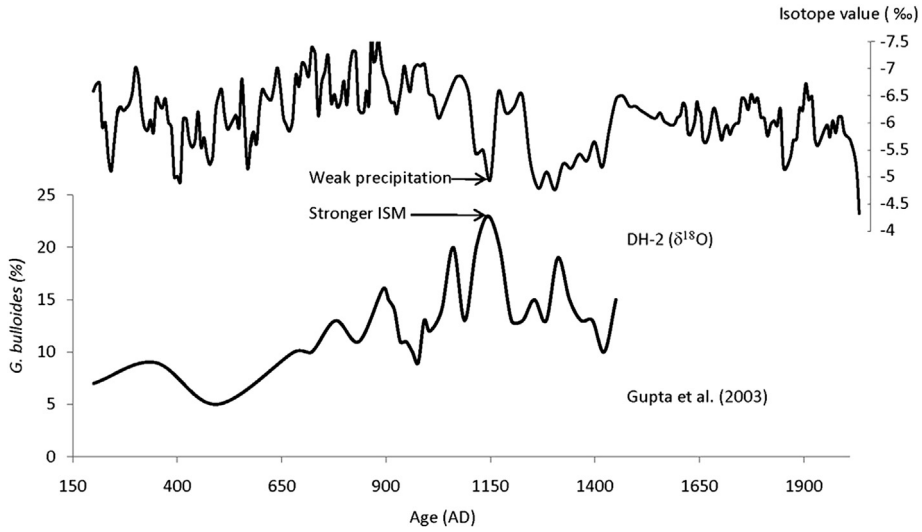

Fig. 8. Comparisons of DH-2 results with Arabian Sea core of Gupta et al. (2003). Episodes of lighter $\delta^{18}O$ values (=higher precipitation) in DH-2 (upper curve) do not show positive correlation with higher *G. bulloides* percentage (=intense ISM) in lower curve, because of the additional role of Westerlies in the Himalayan foothills.

The isotopic record of Kotlia et al. (2012) is consistent with a number of past studies in regions, influenced by both the summer monsoon and Westerlies (see also Wu et al., 2004; Chen et al., 2010; Zhao et al., 2010), although controlled solely by the summer monsoon. This hypothesis may further be strengthened by correlating this study's results with those obtained from a high resolution Holocene core (Gupta et al., 2003) from the Arabian Sea, a site influenced only by the ISM. Gupta et al. (2003) linked the episodes of higher *Globigerina bulloides* directly with the intense ISM upwelling. As expected, large-scale climatic patterns of both the Himalayan and Arabian Sea sites do not show a positive correlation (Fig. 8).

From a higher Himalayan peat profile (30°03′N; Phadtare and Pant, 2006), an abrupt rise in moisture at ~1610 AD (within the age uncertainty) has been noted, similar to the DH-2 record around 1700 AD during the LIA. The expansion of anthropogenic activity, most likely due to agriculture and farming from ~1800 AD onwards, is evident by an increase in the cultural taxa, particularly *Cerealia*-type in the nearby area around Nainital (Gupta, 2008). Multi-decadal rainfall and other multi-proxy data from a number of sites in the Indo-Pacific region clearly suggest wetter climate during the LIA (Newton et al., 2006; Liu et al., 2008; Oppo et al., 2009; Tierney et al., 2010).

The LIA appears to have affected both Northern and Southern Hemispheres, but perhaps not in a globally synchronous mode (Grove, 1988; Bradley, 1992; Bradley and Jones, 1993). The MWP and LIA were also not synchronous all over the globe. In these records, the imprints of the MWP period (generally between 800 and 1200 AD) (see Broecker, 2001) only show a little variation in warmth and hence seem to indicate a regional rather than a global event. The records show comparatively drier post-LIA conditions from 1880 AD onwards. A study of tree rings from a nearby area in the province (see locality 5 in Fig. 1) indicates the lowest precipitation during 1932–1941 AD (Singh and Yadav, 2005), which may coincide with the post-LIA. Sontakke and Singh (1996) extended the all- India summer rainfall (AISR) record from 1813 AD and showed that the middle of the nineteenth century was overall the driest in India.

7. Conclusion

The $\delta^{18}O$ and $\delta^{13}C$ measurements and U/Th dating of stalagmite DH-2 reveal a series of climatic fluctuations during the last ~1800 years in the eastern Kumaun Himalaya. The $\delta^{18}O$ variations reveal six major stages: (1) a phase of gradual increase in the wetter conditions from ~210 to 810 AD and punctuated by three multi-decadal dry events, (2) about a century scale wettest period between ~830 and 910 AD, coinciding with the lower part of the MWP and comparatively higher growth rate of the stalagmite, (3) wetter/warmer MWP from ~830 to 1210 AD with a drier event towards the end, (4) an extremely dry event at ~1080 to 1160 AD, (5) a wetter/warmer or sub-tropical climate during the LIA from ~1440 to 1880 AD, and (6) a drier period from ~1880 AD onwards. Of the dry events, two are more than a century long. The highest precipitation is registered during the lower part of the so-called MWP, corresponding to higher growth rate, whereas, the lowest precipitation is recorded immediately after the termination of MWP, that can perhaps be correlated with the lowest growth rate in the sample. The annual growth of the stalagmite was further accelerated during the LIA under wetter conditions. The wetness in the LIA may be explained as due to the stronger Westerlies in the foothills of the Indian Himalaya during this period.

The precipitation pattern across the South Asian domain is different during a "break monsoon" (Krishnan et al., 2000; Gadgil and Joseph, 2003; Joseph and Sijikumar, 2004; Staubwasser and Weiss, 2006). The behavior of ISM convection and surface winds are changed, resulting in drought periods in southern India but stronger precipitation over the Himalaya and foothills (Staubwasser and Weiss, 2006). The persistent spatial variations of rainfall distribution on the Indian land mass as well as the Himalaya, as today, seem to have been occurring since the Holocene. The northeastern Tibetan Plateau experienced slight warming from 1150 to 1350 AD, while the southern Tibetan Plateau witnessed a dramatic warming from 1150 to 1400 AD (Bao et al., 2003) which indicates that the Late Holocene events may not be synchronous. There may be a need to re-define these anomalies in terms of timing and spatial structure (e.g., Holmes et al., 2009) considering the latitudes, elevations and vegetation zones of different sites in different regions. At least, a clear latitudinal variation in precipitation may be ascribed to the rapid southward migration of the ITCZ (e.g., Newton et al., 2006; Kotlia et al., 2012).

The abrupt centennial ISM events from Arabian Sea through Holocene (Gupta et al., 2003) do not match with this record (see Fig. 8), largely because of the additional role of the Westerlies in the Himalaya. Following Tripathi et al. (2004) that the Himalayan region received greater rainfall than in other parts of India during the Late Holocene, this was due to the stronger Westerlies in the Himalaya and not entirely because of the decrease in the ISM in the Peninsular India. Therefore, the ISM declined and the Westerlies became stronger over the Himalayan foothills during the Late Holocene.

Acknowledgments

The study was financed by DST SERC Fast Track Scheme (No. SR/FTP/ES-97/2009) awarded to JS, and AvH Linkage (3-4-Fokoop, DEU/1017420) and ISRO-GBP (Ahmedabad) projects to BSK. Laboratory facilities were provided by the National Geophysical Research Institute (Hyderabad), University of Melbourne (Australia) and Indian Institute of Science (Bangalore). We are grateful to W. Raza and M. Lone for helping in isotopic measurements and to Dr. J. Fohlmeister, Heidelberg Academy of Sciences for StalAge. We thank Drs. J. Hellstrom and J. Woodhead for providing U/Th dates with the financial support by Australia–India Strategic Research Fund. Special thanks are due to two anonymous reviewers whose constructive and critical comments greatly helped in improving the manuscript.

References

Ahmad, S.M., Babu, A., Padmakumari, G.V.M., Waseem, R., 2008. Surface and deep water changes in the northeast Indian Ocean during the last 60 ka inferred from carbon and oxygen isotopes of planktonic and benthic foraminifera. Palaeogeography, Palaeoclimatology, Palaeoecology 262, 182–188.

Alford, D., 1992. Hydrological Aspects of the Himalayan Region. ICIMOD Occasional Paper 18. International Centre for Integrated Mountain Development, Kathmandu, Nepal.

Anderson, D.M., Overpeck, J.T., Gupta, A.K., 2002. Increase in the Asian southwest monsoon during the past four centuries. Science 297, 596–599.

Baker, A., Smart, P.L., Ford, D.C., 1993. Northwest European paleoclimate as indicated by growth frequency variations of secondary calcite deposits. Palaeogeography, Palaeoclimatology, Palaeoecology 100, 291–301.

Banner, J.L., Guilfoyle, A., James, E.W., Stern, L.A., Musgrove, M., 2007. Seasonal variations in modern speleothem calcite growth in Central Taxas, U.S.A. Journal of Sedimentary Research 77, 615–622. http://dx.doi.org/10.2110/jsr.2007.065.

Bao, Y., Brauning, A., Yafeng, S., 2003. Late Holocene temperature fluctuations on the Tibetan Plateau. Quaternary Science Reviews 22 (21), 2335–2344.

Bradley, R.S., 1992. When was the "Little Ice Age"? In: Mikami, T. (Ed.), Proceedings of the International Symposium on the Little Ice Age Climate. Tokyo Metropolitan University, Tokyo, pp. 1–4.

Bradley, R.S., Jones, P.D., 1993. 'Little Ice Age' summer temperature variations: their nature and relevance to recent global warming trends. The Holocene 3, 367–376.

Briffa, K.R., 2000. Annual climate variability in the Holocene: interpreting the message of ancient trees. Quaternary Science Reviews 19, 87–105.

Broecker, W.S., 2001. Was the medieval warm period global? Science 291, 1497–1499.

Chakraborty, S., Bhattacharyya, S.K., Ranhotra, P.S., Bhattacharyya, A., Bhushan, R., 2006. Palaeoclimatic scenario during Holocene around Sangla valley, Kinnaur, northwest Himalaya based on multi-proxy records. Current Science 91, 777–782.

Chauhan, M.S., 2006. Late Holocene vegetation and climate change in the alpine belt of Himachal Pradesh. Current Science 91, 1562–1567.

Cerling, T.E., 1984. The stable isotopic composition of modern soil carbonate and its relationship to climate. Earth and Planetary Science Letters 71, 229–240.

Chen, F., Holmes, J., Wünnemann, B., Yu, Z., 2009. Holocene climate variability in arid Asia: nature and mechanisms. Quaternary International 194, 1–5.

Chen, F.H., Huang, X.Z., Zhang, J.W., Holmes, J.A., Chen, J.H., 2006. Humid Little Ice Age in arid central Asia documented by Bosten lake, Xinjiang, China. Science in China (Series D) 49, 1280–1290.

Chen, G., Plumb, R.A., Lu, J., 2010. Sensitivities of zonal mean atmospheric circulation to SST warming in an aqua planet model. Geophysical Research Letters 37, L12701.

Chen, J., Wan, G., Zhang, D.D., Chen, Z., Xu, J., Xiao, T., Huang, R., 2005. The 'Little Ice Age' recorded by sediment chemistry in lake Erhai, southwest China. The Holocene 15, 925–931.

Cheng, H., Adkins, J., Edwards, R.L., Boyle, E.A., 2000. U-Th dating of deep-sea corals. Geochimica et Cosmochimica Acta 64, 2401–2416.

Chu, G., Liu, J., Sun, Q., Lu, H., Gu, Z., Wang, W., Liu, T., 2002. The 'Mediaeval warm period' drought recorded in lake Huguangyan, tropical South China. The Holocene 12, 511–516.

Cook, E.R., Krusic, P.J., Jones, P.D., 2003. Dendroclimatic signals in long tree-ring chronologies from the Himalayas of Nepal. International Journal of Climatology 23 (7), 707–732.

Crowley, T.J., Lowery, T.S., 2000. Northern Hemisphere temperature reconstruction. Ambio 29, 51–54.

Daëron, M., Guo, W., Eiler, J., Genty, D., Blamart, D., Boch, R., Drysdale, R., Maire, R., Wainer, K., Zanchetta, G., 2011. ^{13}C ^{18}O clumping in speleothems: observations from natural caves and precipitation experiments. Geochimica et Cosmochimica Acta 75, 3303–3317.

D'Arrigo, R., 2006. On the long-term context for late twentieth century warming. Journal of Geophysical Research 111 (D03 103), 1–12.

Denniston, R.F., Gonzalez, L.A., Asmerom, Y., Sharma, R.H., Reagan, M.K., 2000. Speleothem evidence for changes in Indian summer monsoon precipitation over the last ~2300 years. Quaternary Research 53 (2), 196–202.

Diaz, H.F., Trigo, R., Hughes, M.K., Mann, M.E., Xoplaki, E., Barriopedro, D., 2011. Spatial and temporal characteristics of climate in medieval times revisited. American Meteorological Society (BAMS), 1487–1500. http://dx.doi.org/10.1175/BAMS-D-10-05003.1.

Dorale, J.A., Liu, Z., 2009. Limitations of Hendy test criteria in judging the paleoclimatic suitability of speleothems and the need for replication. Journal of Cave and Karst Studies 71, 73–80.

Dreybrodt, W., 2008. Evolution of the isotopic composition of carbon and oxygen in a calcite precipitating H_2O-CO_2-$CaCO_3$ solution and the related isotopic composition of calcite in stalagmites. Geochimica et Cosmochimica Acta 72, 4712–4724.

Esper, J., Cook, E.R., Schweingruber, F.H., 2002. Low frequency signals in long tree-ring chronologies for reconstructing past temperature variability. Science 295, 2250–2253.

Fleitmann, D., Burns, S.J., Neff, U., Mudelsee, M., Mangini, A., Matter, A., 2004. Palaeoclimatic interpretation of high-resolution oxygen isotope profiles derived from annually laminated speleothems from Southern Oman. Quaternary Science Reviews 23, 935–945.
Gadgil, S., Joseph, P.V., 2003. On breaks of the Indian monsoon. Proceedings of the Indian Academy of Sciences: Earth and Planetary Sciences 112 (4), 529–558.
Gascoyne, M., 1992. Palaeoclimate determination from cave calcite deposits. Quaternary Science Reviews 11 (6), 609–632.
Gasse, F., Fontes, J.C., Van Campo, E., Wei, K., 1996. Holocene environmental changes in Bangong Co basin (Western Tibet). Part 4: discussion and conclusions. Palaeogeography, Palaeoclimatology, Palaeoecology 120, 79–92.
Genty, D., Baker, A., Vokal, B., 2001. Intra-and inter-annual growth rate of modern stalagmites. Chemical Geology 176, 191–212.
Grove, J.M., 1988. The Little Ice Age. Methuen, London, p. 498.
Gupta, A., 2002. Palaeovegetation and past climate of Late Holocene from temperate zone in Naini Tal district, Kumaun Himalaya. Acta Palaeontologica Sinica 41 (4), 517–523.
Gupta, A., 2008. Late Quaternary vegetation and climate from temperate zone of the Kumaun Himalaya, India (with remarks on neotectonic disturbance). Acta Palaeobotanica 48 (2), 325–333.
Gupta, A., Anderson, D.M., Overpeck, J.T., 2003. Abrupt changes in the Asian southwest monsoon during the Holocene and their links to the North Atlantic Ocean. Nature 421, 354–357.
Hegerl, G.C., Thomas, J., Crowley, T.J., Allen, M., Hyde, W.T., Pollack, H.N., Smerdon, J., Zorita, E., 2007. Detection of human influence on a new validated 1500-year temperature reconstruction. Journal of Climate 20, 650–666.
Hellstrom, J., 2003. Rapid and accurate U/Th dating using parallel ion counting multi-collector ICP-MS. Journal of Analytical Atomic Spectrometry 18, 1346–1351.
Hellstrom, J., 2006. U-Th dating of speleothems with high initial ^{230}Th using stratigraphical constraint. Quaternary Geochronology 1, 289–295.
Hendy, C.H., 1971. The isotopic geochemistry of speleothems-1. The calculation of the effects of different modes of formation on the isotopic composition of speleothems and their applicability as paleoclimatic indicators. Geochimica et Cosmochimica Acta 35, 801–824.
Hendy, C.H., Wilson, A.T., 1968. Palaeoclimatic data from speleothems. Nature 219, 48–51.
Holmes, J.A., Cook, E.R., Yang, B., 2009. Climate change over the past 2000 years in western China. Quaternary International 194, 91–107.
Hughes, M.K., Diaz, H.F., 1994. Was there a 'Medieval Warm Period', and if so, where and when? Climate Change 26, 109–142.
Jones, P.D., Briffa, K.R., Barnett, T.P., Tett, S.F.B., 1998. High-resolution palaeoclimatic records for the last millennium: interpretation, integration and comparison with general circulation model control-run temperatures. The Holocene 8, 455–471.
Jones, P.D., Mann, M.E., 2004. Climate over past millennia. Review of Geophysics 42, 1–42.
Joseph, P.V., Sijikumar, S., 2004. Intraseasonal variability of the low-level jet stream of the Asian summer monsoon. Journal of Climate 17, 1449–1458.
Juckes, M.N., Allen, M.R., Briffa, K.R., Esper, J., Hegerl, G.C., Moberg, A., Osborn, T.J., Weber, S.L., 2007. Millennial temperature reconstruction intercomparison and evaluation. Climate of the Past 3, 591–609.
Jung, S.J.A., Davies, G.R., Ganssen, G.M., Kroon, D., 2004. Synchronous Holocene sea surface temperature and rainfall variations in the Asian monsoon system. Quaternary Science Reviews 23, 2207–2218.
Kar, R., Ranhotra, P.S., Bhattacharyya, A., Sekar, B., 2002. Vegetation vis-a-vis climate and glacial fluctuations of the Gangotri glacier since the last 2000 years. Current Science 82, 347–351.
Kaufmann, G., Dreybrodt, W., 2004. Stalagmite deposition and paleo-climate: an inverse approach. Earth and Planetary Science Letters 224, 529–545.
Kotlia, B.S., Ahmad, S.M., Zhao, J.X., Raza, W., Collerson, K.D., Joshi, L.M., Sanwal, J., 2012. Climatic fluctuations during the LIA and post-LIA in the Kumaun Lesser Himalaya, India: evidence from a 400 yr old stalagmite record. Quaternary International 263, 129–138.
Kotlia, B.S., Sanwal, J., Phartiyal, B., Joshi, L.M., Trivedi, A., Sharma, C., 2010. Late Quaternary climatic changes in the eastern Kumaun Himalaya, India, as deduced from multi-proxy studies. Quaternary International 213, 44–55.
Krishnan, R., Zhang, C., Sugi, M., 2000. Dynamics of breaks in the Indian summer monsoon. Journal of Atmospheric Sciences 57, 1354–1372.
Liu, X.Q., Dong, H.L., Rech, J.A., Matsumoto, R., Yang, B., Wang, Y.B., 2008. Evolution of Chaka Salt Lake in NW China in response to climatic change during the latest Pleistocene-Holocene. Quaternary Science Reviews 27, 867–879.
Ljungqvist, F.C., 2010. A new reconstruction of temperature variability in the extra-tropical Northern Hemisphere during the last two millennia. Swedish Society for Anthropology and Geography 92, 339–351.
Loehle, C., 2007. A 2000-year global temperature reconstruction based on non-tree ring proxies. Energy and Environment 18 (7–8), 1049–1058.
Mann, M.E., Bradley, R.S., Hughes, M.K., 1999. Northern Hemisphere temperatures during the past millennium: inferences, uncertainties and limitations. Geophysical Research Letters 26, 759–762.
Mann, M.E., Zhang, Z., Hughes, M.K., Bradley, R.S., Miller, S.K., Rutherford, S., Ni, F., 2008. Proxy-based reconstructions of hemispheric and global surface temperature variations over the past two millennia. Proceedings of the National Academy of Sciences 105, 13252–13257.
Mann, M.E., Zhang, Z., Rutherford, S., Bradley, R.S., Hughes, M.K., Shindell, D., Ammann, C., Faluvegi, G., Ni, F., 2009. Global signatures and dynamical origins of the Little Ice Age and Medieval climate anomaly. Nature 326, 1256–1260.
Mann, M.E., Jones, P.D., 2003. Global surface temperatures over the past two millennia. Geophysical Research Letters 30, 1–5.
McDermott, F., 2004. Palaeo-climate reconstruction from stable isotope variations in speleothems: a review. Quaternary Science Reviews 23, 901–918.
Mickler, P.J., Banner, J.L., Stern, L., Asmerom, Y., Edwards, R.L., Ito, E., 2004. Stable isotope variations in modern tropical speleothems: evaluating equilibrium vs. kinetic isotope effects. Geochimica et Cosmochimica Acta 68, 4381–4393.
Mickler, P.J., Stern, L.A., Banner, J.L., 2006. Large kinetic isotope effects in modern speleothems. Geological Society of America Bulletin 118, 65–81.
Moberg, A., Sonechkin, D.M., Holmgren, K., Datsenko, N.M., Karlen, W., 2005. Highly variable Northern Hemisphere temperatures reconstructed from low- and high-resolution proxy data. Nature 433, 613–617.
Newton, A., Thunell, R., Stott, L., 2006. Climate and hydrographic variability in the Indo-Pacific Warm Pool during the last millennium. Geophysical Research Letters 33, L19710. http://dx.doi.org/10.1029/2006GL027234.
Oppo, D.W., Rosenthal, Y., Linsley, B.K., 2009. 2,000-year-long temperature and hydrology reconstructions from the Indo-Pacific warm pool. Nature 460, 1113–1116.
Osborn, T., Briffa, K., 2006. Spatial extent of 20th century warmth in the context of the past 1200 years. Science 311, 841–844.
Osmond, C.B., Ziegler, H., 1975. Schwere pflanzen and leichte pfanzen: stable isotope in photosynthesis toffwechel un in der biochemischen okaklogie. Narturwissenschaft Rundschau 28, 1–323.
Overpeck, J.T., Anderson, D., Trumbore, S., Prell, W., 1996. The southwest Indian Monsoon over the last 18000 yrs. Climate Dynamics 12, 213–225.
Overpeck, J.T., Sturm, M., Francis, J.A., Perovich, D.K., Serreze, M.C., Benner, R., Carmack, E.C., Chapin III, F.S., Gerlach, S.C., Hamilton, L.C., Hinzman, L.D., Holland, M., Huntington, H.P., Key, J.R., Lloyd, A.H., MacDonald, G.M., McFadden, J., Noone, D., Prowse, T.D., Schlosser, P., Vörösmarty, C., 2005. Arctic system on trajectory to new, seasonally ice-free state. EOS 86 (34), 309–313.
Phadtare, N.R., 2000. Sharp decrease in summer monsoon strength 4000–3500 cal yr BP in the central higher Himalaya of India based on pollen evidence from alpine peat. Quaternary Research 53, 122–129.
Phadtare, N.R., Pant, R.K., 2006. A century-scale pollen record of vegetation and climate history during the past 3500 years in the Pinder Valley, Kumaon Higher Himalaya, India. Journal of Geological Society of India 68, 495–506.
Prasad, S., Kusumgar, S., Gupta, S.K., 1997. A mid to late Holocene record of palaeoclimatic changes from Nal Sarovar: a palaeodesert margin lake in western India. Journal of Quaternary Science 12, 153–159.
Ranhotra, P.S., Bhattacharyya, A., Kar, R., Sekar, B., 2001. Vegetation and Climatic Changes Around Gangotri Glacier During Holocene. Geological Survey of India, Special Publication 65, pp. 67–71.
Rawat, S., Phadtare, N.R., Sangode, S.J., 2012. The Younger Dryas cold event in NW Himalaya based on pollen record from the Chandra Tal area in Himachal Pradesh, India. Current Science 102 (8), 1193–1198.
Rühland, K., Phadtare, N.R., Pant, R.K., Sangode, S.J., Smol, J.P., 2006. Accelerated melting of Himalayan snow and ice triggers pronounced changes in a valley peatland from northern India. Geophysical Research Letters 33, L 15709. http://dx.doi.org/10.1029/2006GL026704.
Sarkar, A., Ramesh, R., Somayajulu, B.L.K., Agnihotri, R., Jull, A.J.T., Burr, G.S., 2000. High resolution Holocene monsoon record from the eastern Arabian Sea. Earth and Planetary Science Letters 177, 209–218.
Scholz, D., Hoffmann, D.L., 2011. StalAge-an algorithm designed for construction of speleothem age models. Quaternary Geochronology 6, 369–382.
Schulz, H., von Rad, U., Erlenkeuser, H., 1998. Correlation between Arabian Sea and Greenland climate oscillations of the past 11,000 years. Nature 393, 54–57.
Schwarcz, H.P., 1986. Geochronology and isotope geochemistry in speleothems. In: Fritz, P., Fontes, J. (Eds.), Handbook of Environmental Isotope Geochemistry. Elsevier, Amsterdam, pp. 271–303.
Sharma, C., Gupta, A., 1995. Vegetational history of Nachiketa Tal, Garhwal Himalaya, India. Journal of Nepal Geological Society 10, 29–34.
Sharma, C., Gupta, A., 1997. Vegetation and climate in Garhwal Himalaya during Early Holocene. Palaeobotanist 46, 111–116.
Singh, J., Yadav, R., 2005. Spring precipitation variations over the western Himalaya, India, since A.D. 1731 as deduced from tree rings. Journal of Geophysical Research 110, D01110. http://dx.doi.org/10.1029/2004JD004855.
Sinha, A., Cannariato, K.G., Stott, L.D., Li, H.C., You, C.F., Cheng, H., Edwards, R.L., Singh, I.B., 2005. Variability of Southwest Indian summer monsoon precipitation during the Bølling-Allerød. Geology 33 (10), 813–816.
Sirocko, F., GarbeSchonberg, D., McIntyre, A., Molfino, B., 1996. Teleconnections between the subtropical monsoons and high-latitude climates during the last deglaciation. Science 272, 526–529.
Sirocko, F., Sarnthein, M., Erlenleuser, H., Lange, H., Arnold, M., Duplessy, J.C., 1993. Century-scale events in monsoonal climate over the past 24,000 years. Nature 364, 322–324.
Sontakke, N.A., Singh, N., 1996. Longest instrumental regional and All-India summer monsoon rainfall series using optimum observations: reconstruction and update. The Holocene 6, 315–331.
Spötl, C., Mangini, A., 2002. Stalagmite from the Austrian Alps reveals Dansgaard-Oeschger events during isotope stage 3: implications for the absolute chronology of Greenland ice cores. Earth and Planetary Science Letters 203, 507–518.

Staubwasser, M., Sirocko, F., Grootes, P., Segl, M., 2003. Climate change at the 4.2 ka BP termination of the Indus valley civilization and Holocene south Asian monsoon variability. Geophysical Research Letters 30, 1425. http://dx.doi.org/10.1029/2002GL016822.

Staubwasser, M., Weiss, H., 2006. Holocene climate and cultural evolution in late prehistoric–early historic West Asia. Quaternary Research 66 (3), 372–387.

Stine, S., 1994. Extreme and persistent drought in California and Patagonia during mediaeval time. Nature 369, 546–549.

Talma, A.S., Vogel, J.C., 1992. Late Quaternary paleotemperatures derived from a speleothem from Cango Caves, Cape Province, South Africa. Quaternary Research 37, 203–213.

Tierney, J.E., Oppo, D.W., Rosenthal, Y., Russell, J.M., Linsley, B.K., 2010. Coordinated hydrological regimes in the Indo-Pacific region during the past two millennia. Paleoceanography 25 (PA1102), 7.

Tripathi, J.K., Bock, B., Rajamani, V., Eisenhauer, A., 2004. Is river Ghaggar, Saraswati? Geochemical constraints. Current Science 87, 1141–1145.

Valdiya, K.S., 1980. Geology of Kumaun Lesser Himalaya. Wadia Institute of Himalayan Geology Publication, p. 294.

Webster, J.W., Brook, G.A., Railsback, L.B., Cheng, H., Edwards, R.L., Alexander, C., Reeder, P.P., 2007. Stalagmite evidence from Belize indicating significant droughts at the time of pre-classic abandonment, the Maya hiatus, and the classic Maya collapse. Palaeogeography, Palaeoclimatology, Palaeoecology 250, 1–17.

Woo, K.S., Jo, K., Edwards, L.R., Cheng, H., Wang, Y., Yoon, H., 2006. Kinetic fractionation processes recorded in the stalagmites of some limestone caves in Korea. American Geophysical Union, Fall Meeting. Abstract PP51D-1160.

Wu, G.X., Liu, Y., Mao, J., Liu, X., Li, W., 2004. Adaptation of the atmospheric circulation to thermal forcing over the Tibetan Plateau. In: Zhu, X., et al. (Eds.), Observation, Theory and Modeling of Atmospheric Variability. Selected Papers of Nanjing Institute of Meteorology Alumni in Commemoration of Professor Jijia Zhang. World Scientific, pp. 92–114.

Yang, B., Braeuning, A., Johnson, K.R., Yafeng, S., 2002. General characteristics of temperature variation in China during the last two millennia. Geophysical Research Letters 29. http://dx.doi.org/10.1029/2001GL014485.

Zhang, Y., Kong, Z.C., Yan, S., Yang, Z.J., Ni, J., 2009. "Medieval warm period" on the northern slope of central Tianshan mountains, Xinjiang, NW China. Geophysical Research Letters 36, L11702. http://dx.doi.org/10.1029/2009GL037375.

Zhao, P., Cao, Z.H., Chen, J.M., 2010. A summer teleconnection pattern over the extratropical Northern Hemisphere and associated mechanisms. Climate Dynamics 35, 523–534.

Zhou, H., Zhao, J., Qing, W., Feng, Y., Tang, J., 2011. Speleothem-derived Asian summer monsoon variations in Central China, 54–46 ka. Journal of Quaternary Science 26, 781–790.